European Review for Medical and Pharmacological Sciences 2020; 24: 12912-12928

Effect and mechanism of miR-135a-5p/CXCL12/JAK-STAT axis on inflammatory response after myocardial infarction

X.-Y. GUO, Q.-L. LIU, W. LIU, J.-X. CHENG, Z.-J. LI

Department of Cardiology, The First Affiliated Hospital, and College of Clinical Medicine of Henan University of Science and Technology, Luoyang, Henan Province, P.R. China

Abstract. – OBJECTIVE: To investigate the regulatory role of miR-135a-5p/CXCL12/JAK-STAT signaling axis in inflammatory response after myocardial infarction (MI).

MATERIALS AND METHODS: With the construction of mouse model with MI by ligation of left descending coronary artery, modeling mice were subdivided into sh-NC group, sh-CXCL12 group, agomir-NC group, miR-135a-5p agomir group and miR-135a-5p-agomir+pcDNA-CXCL12 with intravenous injection of corresponding adenovirus, and no modeling was made for mice in the sham operation group. Simulation of MI *in vivo* was realized by hypoxia model *in vitro*, with the establishment of groups including mimic-NC group, miR-135a-5p mimic group, inhibitor-NC group, miR-135a-5p inhibitor group, sh-NC group, sh-CXCL12 group, oe-NC group, oe-CXCL12 group, mimic NC+oe-NC group, miR-135a-5p mimic+oe-NC group, and miR-135a-5p mimic+oe-CXCL12 group. Real-time quantitative polymerase chain reaction (qRT-PCR) was used to detect the level of miR-135a-5p, CXCL12, TNF-α, IL-1β and IL-6, and Western blot were further performed to detect the mRNA and protein expression of JAK2/p-JAK2 and STAT3/p-STAT3, respectively. Hematoxylin-eosin (HE) staining and terminal deoxynucleotidyl transferase-mediated dUTP-biotin nick end labeling (TUNEL) assay were used to evaluate MI in mice. Dual-Luciferase reporter assay was used to verify the targeting relationship between miR-135a-5p and CXCL12. Annexin V-fluorescein isothiocyanate/propidium iodide (V-FITC/PI) double staining analysis by flow cytometry was used to detect apoptosis.

RESULTS: After hypoxia of myocardial cell line H9c2 for 24 h, there were increased expression of CXCL12, decreased expression of miR-135a-5p, increased number of apoptotic cells, as well as upregulated levels of TNF-α, IL-1β and IL-6 (all $p<0.05$). Meanwhile, similar results were found in the myocardial tissues. Dual-Luciferase reporter assay indicated that miR-135a-5p could target the expression of CXCL12. Transfection of miR-135a-5p mimic or sh-CXCL12 could reduce the number of apoptotic myocardial cells and inhibit the level of TNF-α, IL-1β and IL-6 (all $p<0.05$). Furthermore, miR-135a-5p mimic or sh-CXCL12 could result in the suppressed expression of p-JAK2 and p-STAT3 (all $p<0.05$). Compared with miR-135a-5p mimic +DMSO group, the expression of JAK2 and STAT3 in miR-135a-5p mimic +RO8191 group had no significant change ($p>0.05$); the expression of p-JAK2 and p-STAT3 was increased (all $p<0.05$), suggesting that miR-135a-5p negatively regulated the expression of CXCL12 and inhibited the activation of JAK-STAT signaling pathway. In addition, for further verification, experiments carried out in sh-NC group, sh-CXCL12 group, agomir-NC group and miR-135a-5p agomir group found that sh-CXCL12 and miR-135a-5p agomir resulted in decreased area of MI decreased, the number of apoptotic cells, the expression of p-JAK2 and p-STAT3 (all $p<0.05$); while compared with miR-135a-5p-agomir group, miR-135a-5p-agomir+pcDNA-CXCL12 group showed increased area of MI decreased, the number of apoptotic cells, the expression of p-JAK2 and p-STAT3 (all $p<0.05$).

CONCLUSIONS: Inhibition of miR-135a-5p/CXCL12/JAK-STAT signaling axis can reduce inflammatory reaction and apoptosis after MI, and hence contribute to the improvement of the degree of myocardial injury.

Key Words:
MiR-135a-5p, CXCL12, Myocardial infarction, Inflammatory reaction, Cell apoptosis, Hypoxia.

Introduction

Myocardial infarction (MI) is a type of myocardial ischemic necrosis caused by rapid decrease or interruption of coronary artery blood

Corresponding Author: ZhiJuan Li, MM; e-mail: 13838836086@126.com

supply, resulting in severe and persistent myocardial ischemia[1]. It can lead to the persistent necrosis of the distal myocardium of the infarct area[2]. The infarct site is consistent with the coronary artery blood supply area, most of which occurs in the left ventricle, and the early stage of post-MI is mainly inflammatory reaction[3]. It is found that there is abnormal expression of cardiac microRNA (miRNA) in patients with MI, which may become a new marker and therapeutic target of MI[4]. MiRNA is an endogenous non coding single stranded RNA, which contains 19-22 nucleotides[5]. It can degrade or inhibit the translation of target mRNA through specific binding with 3′UTR of target mRNA, so as to regulate gene post transcription[6]. At present, the majority of past studies on miRNAs are focused on tumors, and specific miRNAs can participate in the growth of tumor cells[7,8]. However, the research on the role and regulation mechanism of miRNAs in heart disease is developing. With the deepening of research, miRNAs are expected to become a new generation of biomarkers and auxiliary diagnostic tools for cardiovascular diseases, and even become a new target for prevention and treatment of such diseases[9,10]. It has been reported that miRNA has a regulatory effect on inflammation, and miR-135a-5p has been involved in autophagy and inflammation related research in a CCI model of neuropathic pain[11]. Besides, the related research in the aspect of inflammation is rare, especially the study of miR-135a-5p in the regulation of inflammation after MI has not been carried out.

Chemokine CXCL12, also known as stromal cell-derived factor-1 or pre-B cell stimulating factor, belongs to the CXC chemokine family[12]. It is a kind of cytokine secreted by leukocytes and has chemotaxis[13]. It can induce inflammatory reaction by driving and regulating the expression of adhesion molecules and (or) directly chemotaxing and attracting inflammatory cells through some undetermined pathways[14]. Therefore, it plays an important role in immune defense, anti-infection and inflammatory reaction[15,16]. Previous studies have showed that the expression of CXCL12 in patients with unstable angina pectoris and MI is significantly increased[17,18]. In addition, a variety of different cellular signaling pathways play an important role in a series of pathophysiological changes after MI[19]. They are activated by different factors such as inflammation, and the activation of related signaling pathways can produce myocardial protection through various downstream cytokines or further aggravate myocardial injury[20]. Therefore, a hypothesis is proposed in this study whether it is possible to reduce some cytokines that play a key role in the inflammatory response after MI by regulating certain signaling pathway. It may provide a reference for the protection of heart function after MI and alleviate or avoid heart failure.

Various signaling pathways are involved significantly in the development processes of MI, such as cell differentiation and division. Pathways such as Wnt, PTEN/PI3K/Akt, ERK/MAPK, etc. are common ones that have important roles in explaining the underlying mechanisms and exert therapeutic effects in cardiac repairing, and hence producing cardioprotective role and MI healing function[21-23]. Among them, Janus kinase/signal transducer and activator of transcription pathway (JAK-STAT) is a type of intracellular signal transduction pathway with interferon-like effect, which actively participates in many physiological and pathophysiological processes, such as immune regulation, cell proliferation and differentiation, apoptosis, inflammation, tumorigenesis, etc.[24,25]. Activated JAK phosphorylates the specific tyrosine residues on the receptor, making it become the binding site of stat and other intracellular signal molecules[26]. The STAT gathered at this site is phosphorylated and activated under the action of JAK[27]. The activated STAT further separates from the receptor, forms dimer and transfers into the nucleus, thus starting the corresponding target gene transcription[28]. JAK-STAT signaling pathway is an important pathway of cytokine signal transduction, which is closely related to a variety of cardiovascular diseases, such as myocardial hypertrophy, heart failure, myocardial ischemic preconditioning, acute MI, ischemia/reperfusion injury after MI, etc.[29-31].

At present, there is accumulated understanding on the effect of JAK-STAT signaling pathway and the role of some miRNAs in ischemia/reperfusion injury, myocardial ischemic preconditioning, hypertensive myocardial hypertrophy and viral myocarditis. However, the regulation of miR-135a-5p/CXCL12/JAK-STAT signaling axis in the inflammatory response and cell apoptosis after MI is still blank in China and rarely reported abroad. Therefore, it will be a meaningful and worth studying topic, and our study emphasizes on clarifying this issue.

Materials and Methods

Construction and Identification of Mouse Model of MI

Ninety SPF grade C57BL/6J mice, aged 6-8 weeks, weighing 20-25 g, were selected as the objects of study. Ten mice were randomly selected as the normal control group, and the remaining 80 were used to construct the MI model in mice. All mice were fed in SPF animal laboratory with humidity of 60%-65% and temperature of 23-25°C. All mice were given normal diet. Experimental procedures related in this study have been approved by the Local Animal Ethics Committee of the First Affiliated Hospital.

After successful intraperitoneal injection of 1% Pentobarbital Sodium (50 mg/kg), the skin of the front neck and left chest was prepared, the limbs were fixed, the chest was facing the light source, the tongue was pulled out moderately, and the larynx with the movement of opening and closing was the trachea. At this time, the appropriate cannula with needle core was inserted, the needle core was pulled out, and the mouse was supine on the operating board. The intubation was connected to the ventilator. The inspiratory to expiratory ratio of respiratory parameters was set at 1:1.5, the respiratory rate was about 130 times/min, and the tidal volume was about 1.0 ml. The tracheal intubation was successful when the respiratory rate of the mice was consistent with that of the ventilator. The left chest was fully exposed (the chest hair was scraped off in advance), and the skin, muscle tissue and other tissues in this region were cut in the fourth intercostal space of the left chest to expose the heart. Under the junction of pulmonary artery trunk and left atrial appendage and about 0.1 cm below the lower edge of left atrial appendage, the needle should be inserted through puncture, and it should not be too deep. About 1 min after ligation and suture, it was observed that the anterior wall of left ventricle was pale and the pulsation was weakened due to ligation ischemia, which proved that the ligation was successful. After observing the bleeding situation of the operation field, the thoracic cavity was closed and sutured layer by layer, and the gas of thoracic cavity was aspirated with syringe to form negative pressure. After the recovery of spontaneous breathing, the tracheal intubation was removed, the respiratory tract was cleaned, and the mice were kept warm after operation. The feeding temperature was 23-25°C. In the sham operation group, the abdominal cavity was opened, punctured without ligation and then closed and sutured. Samples were collected 28 d after operation. After anesthetizing the animals (the method described above), the eyeballs of mice were removed with curved forceps, and 0.8-1.5 ml blood was collected with anticoagulant blood collection tube (BD Biosciences, Franklin Lakes, NJ, USA), and then the thoracic cavity was opened to separate the mouse heart. Total RNA was extracted from normal heart tissue and the heart tissue in the marginal zone of MI or fixed with 4% paraformaldehyde for HE staining. To ensure the success rate and reduce the error, the operation of MI model was completed by trained personnel.

In addition to the sham operation group, sh-NC, sh-CXCL12, agomir-negative control (NC), miR-135a-5p agomir, agomir-NC+pcDNA, agomir-NC+pcDNA-CXCL12, and miR-135a-5p-agomir+pcDNA-CXCL12 groups were set up in advance. Each group of adenovirus vector 1×10^9 PFU/mouse) was injected into C57BL/6J mice by tail vein injection.

Culture of Myocardial Cells and Establishment of Cell Model

Mouse myocardial cell line H9c2 cells (Cell Bank of Chinese Academy of Sciences) were used as experimental objects. H9c2 cell culture medium was as follows: fetal bovine serum: high-glucose Dulbecco's Modification of Eagle's Medium (DMEM) and complete culture medium containing 10% fetal bovine serum (FBS) was prepared according to the ratio of 1:9. The cells were cultured at 37°C, 5% CO_2 and saturated humidity incubator. All mouse researches in this study were carried out according to the ethical standards formulated by the experimental Animal Ethics Committee of Tongji University.

The primer sequence of cell transfection was designed and synthesized by Shanghai Borui Biotechnology Co., Ltd. The recombinant adenovirus mediated miR-135a-5p overexpression vector, CXCL12 silent expression recombinant vector and corresponding blank control adenovirus were constructed and packaged by OBIO Biotechnology (Shanghai) Co., Ltd. Cell groups were described as follows: mimic-NC (transfection of negative control plasmid of miR-135a-5p mimic), miR-135a-5p mimic (transfection of miR-135a-5p mimic); inhibitor-NC (transfection of negative control plasmid of miR-135a-5p inhibitor), miR-135a-5p inhibitor (transfection of miR-135a-5p inhibitor); sh-NC (transfection

of negative control plasmid of sh-CXCL12), sh-CXCL12 (transfection of sh-CXCL12 plasmid), oe-NC (transfection of negative control plasmid of oe-CXCL12), oe-CXCL12 (transfection of oe-CXCL12 plasmid); mimic NC+oe-NC (transfection of mimic NC and oe-NC), miR-135a-5p mimic+oe-NC (transfection of miR-135a-5p mimic and oe-NC), miR-135a-5p mimic+oe-CXCL12 (transfection of miR-135a-5p and oe-CXCL12); in addition, JAK2 agonist RO8191 was added for treatment of the myocardial cells after miR-135a-5p mimic treatment, with the establishment of mimic-NC +DMSO group, miR-135a-5p mimic group +DMSO and miR-135a-5p mimic +RO8191 group. In terms of the transfection steps for plasmid, on the day before transfection, 5.0×10^5 cells were inoculated into each well. Antibiotics should not be added to the culture medium, and the transfection was carried out when the cells fused to about 90%. An amount of 1 μg plasmid was diluted with 100 μl serum-free medium and kept for 10 min at room temperature. The 3 μl transfection reagent (Lipofectamine 2000) was diluted to 100 μl with serum-free medium, and the next step was performed within 20 min after standing for 5 min at room temperature. The target plasmids prepared in the first two steps were mixed with the transfection reagent (Lipofectamine 2000), and then incubated at room temperature for 15 min. The adherent cells in the 6-well plate were washed with appropriate serum-free medium to remove the serum contained in the original medium. No serum was found in the medium, which made the cells starved and the transfection efficiency was improved. A serum-free medium was added into each 6-well plate, and 200 μl mixture was added into the 6-well plate well, with each well marked. The culture plate was gently shaken with cross-shaking method to mix the medium. The medium was placed in the incubator with 5% CO_2 at 37°C for 6-8 h. In addition, a microplate containing Opti-MEMI serum-free medium and transfection reagent Lipofectamine 2000 was used as the normal control well. After 6-8 h of transfection, it was replaced with 2 ml Roswell Park Memorial Institute-1640 (RPMI-1640) medium containing I0% fatal bovine serum (FBS). After mixing, the cells were kept in 37°C and 5% CO_2 incubator for 24-48 h for the subsequent experiments. In addition, as for adenovirus transfection, cells at the concentration of about 5.0×10^5 was inoculated into the 6-well place and cultured with DMEM culture medium containing 10% FBS. After that, 1 μl adenovirus working fluid (1×10^8 PFU/ml) was collected and added into the culture medium for further culture. After transfection, cell hypoxia model was established 72 h after transfection to simulate MI model, with corresponding cells in the hypoxia group and control group placed in corresponding culture condition. Subsequent studies were continued after 24 h of culture.

Real-Time Quantitative Polymerase Chain Reaction (qRT-PCR)

Total RNA was extracted by TRIzol reagent. (1) For *in vivo* experiment in tissues, the normal cardiac tissue of the sham operation group and infarct margin tissue of the model group were collected to 1.5 ml EP tube, and 1 ml TRIzol was added to preserve at -80°C. After thawing, 200 μl chloroform was added, shaken upside down, let stand for 3 min, and centrifuged at 4°C for 15 min at 12,000 rpm. The upper water phase was absorbed into a new centrifuge tube. After the above steps, 500 μl isopropanol was added, let stand at room temperature for 10 min, and centrifuged for 5 min at 4°C at 7,500 rpm. An amount of 1 ml 75% ethanol was added and centrifuged at 4°C for 5 min. After air dry for 30 min in in super clean table, the sample was dissolved in 20 μl DEPC solution, and stored at -80°C. (2) For *in vitro* experiment in cells, the following steps were the same as before after the collection of myocardial cells after transfection in each group. Real-time PCR was performed after RNA concentration and quality detection, followed by amplification according to the protocol of SYBR Green Real-time PCR Master Mix. The primers of miR-135a-5p and internal reference U6, as well as CXCL12, TNF-α, IL-1β and IL-6 and internal reference GAPDH (Table I) were completed by Shanghai Jima Pharmaceutical Technology Co.,Ltd. Each gene was repeated in 3 wells in each tube. The following 10 μl system (SYBR 5 μl, Primer mix 1 μl, cDNA 4 μl) was rotated and centrifuged at low speed, and then put into the instrument and pre-denatured at 95°C for 10 min; then denatured at 95°C for 15 s, annealed at 60°C for 60 s, and extended at 72°C for 25 s, in a total of 40 cycles. The specificity of PCR reaction was judged according to the dissolution curve, and the quantitative results were calculated according to the CT value of standard curve and fluorescence curve. The relative expression level was calculated by $2\text{-}\Delta\Delta Ct$ method.

Table I. Primer sequences for qRT-PCR.

Gene names	Primer sequences
miR-135a-5p	F:5'-CCGGCCTATGGCTTTTTATTCC-3' R:5'-CAGTGCAGGGTCCGAGGT-3'
CXCL12	F:5'-CCGCGCTCTGCCTCAGCGACGGGAA-3' R:5'-CTTGTTTAAAGCTTTCTCCAGGTACT-3'
TNF-α	F:5'-TGAGCACAGAAAGCATGATC-3' R:5'-CATCTGCTGGTACCACCAGTT-3'
IL-1β	F:5'-GACCTGTTCTTTGAGGCTGAC-3' R:5'-TCCATCTTCTTCTTTGGGTATTGTT-3'
IL-6	F:5'-GGCCCTTGCTTTCTCTTCG-3' R:5'-ATAATAAAGTTTTGATTATGT-3'
GAPDH	F:5'-AGTGCCAGCCTCGTCTCATA-3' R:5'-GGTAACCAGGCGTCCGATAC-3'
U6	F:5'-GGAACGATACAGAGAAGATTAGC-3' R:5'-TGGAACGCTTCACGAATTTGCG-3'

Note: F: Forward; R: Reverse.

Western Blot

The total protein was extracted by radio immunoprecipitation assay (RIPA). The samples in each group were stored in 1.5 ml Eppendorf (EP) tube with accurate marking and stored at -80°C. The protein concentration was determined by bicinchoninic acid (BCA) kit. In the process of Western blot protein expression detection, the specific steps were as follows: the glue was prepared and then injected. After mixing the prepared separation gel, the gel was injected immediately, and the above calculated protein loading volume was added into the well in turn. In the step of electrophoresis, the voltage of electrophoretic apparatus was adjusted to 80V, about 30 min. After the marker band appeared, the voltage was adjusted to 120V. Pay attention to stop electrophoresis when the bromophenol blue runs near the bottom of separation gel. At the end of film transfer, the NC membrane was taken out to carefully remove the glue on the membrane, observe the band on the membrane and cut the membrane. The membrane was placed into 5% skimmed milk powder (5 g skimmed milk powder added with 100 ml Tris-Buffered Saline and Tween-20 [TBST]), and gently shaken on the shaker for 2 h at room temperature. After that, the diluted primary antibody was added and incubated overnight at 4°C; the next day, the NC membrane was washed with TBST solution for 10 min and repeated 3 times. In the next step, the fluorescent labeled secondary antibody was added and incubated in shaking bed at room temperature for 2 h, after which was three times of washing with TBST (10 min each). GAPDH was used as the internal reference, and the ratio of gray value of target band to internal reference band was used as the relative expression amount of protein. As for scanning and exposure, the Odyssey instrument was used to scan and Image J software system to analyze the image and calculate the gray value. Each group was repeated three times.

Hematoxylin-eosin (HE) Staining

The myocardial tissue of each group was fixed with 4% paraformaldehyde for 1 d, and then paraffin section was made, with thickness of 5 μm. Harris hematoxylin solution and eosin staining were used to observe the changes of cardiac tissue. As for the detailed steps, the paraffin section was roasted at 60°C for 1 h. The next steps were dewaxing and rehydration, the slices were immersed in xylene I, II and III solution for 15 min each; followed by rehydration with ethanol gradient from high to low (100% absolute ethanol I, II → 95% ethanol → 85% ethanol → 75% ethanol), 5 min for each, and washing with double distilled water I, II, 5 min for each. After that, the sections were stained with hematoxylin for 2 min, washed with running water for 10 min, differentiated with 1% hydrochloric acid for 1 s after removed the unfixed dye, washed with running water for 15 min, and rinsing with phosphate-buffered saline (PBS) I and II for 5 min each. Afterwards, it was eosin staining for 5 min, PBS I and II rinsing, 5 min each. Dehydration was the next step, which was performed in the order of 75% ethanol for 5 s → 85% ethanol for 1 min → 95% ethanol for 5 min → 100% ethanol for 5 min → 100% ethanol II for 5 min. Then, transparent processing was conducted by using Xylene I, xylene II and xylene III, 14 min each, followed by sealing with neutral

gum. Finally, the section was observed under ordinary optical microscope (Olympus, Tokyo, Japan).

Terminal Deoxynucleotidyl Transferase-mediated dUTP-biotin Nick End Labeling (TUNEL) Assay

The myocardial tissue of each group was fixed with 4% paraformaldehyde for 1 d, and then paraffin section was made, with a thickness of 5 μm. The detailed steps of TUNEL staining were as follows: The paraffin sections were baked in an oven at 62°C for 2 h; the slices were taken out and put into xylene I, II and III for 15 min each. The next step was rehydration in turn: 100% absolute ethanol I, II → 95% ethanol → 85% ethanol → 75% ethanol → 50% ethanol, 5 min for each, double distilled water I and II for 5 min, PBS for 5 min ×3 times. The tissues were incubated at room temperature for 20 min with 50 μl 20 μg/ml proteinase K working solution. After PBS washing three times (5 min each) to wash proteinase K, in the experimental group, about 50 μl TUNEL reaction solution was added, while in the control group, 50 μl label solution was added and incubated at 37°C for 60 min. The sections were kept away from light and moisturized during the experiment. The number of apoptotic cells was counted under fluorescence microscope.

Dual-Luciferase Reporter Assay

pGL3-CXCL12-3'UTR was constructed by ligation with pGL3-Promoter reporter gene vector digested with Xba I/Hpa I. H9c2 cells were inoculated into 24 well plate and transfected when the cell density reached 80%. The constructed luciferase reporter plasmid CXCL12 (WT, wild type) or mutant (MUT, mutant type) was co-transfected into H9c2 cells with miR-135a-5p mimic or mimic-NC, respectively. They were cultured in serum-free high-glucose DMEM medium and antibiotics, mixed well and reacted at room temperature for 5 min. Each well was replaced with 300 μl fresh serum-free antibiotic-free high-glucose DMEM medium, the mixture was added, evenly mixed and placed in the incubator, cultured at 37°C and 5% CO_2. About 6 h after transfection, the cells were replaced with normal high-glucose DMEM medium. After 24 h of culture, Luciferase activity was determined by Dual-Luciferase reporter gene assay kit. Specifically, the cells were washed with PBS, and 100 μL of cell lysate was added into each well, and the cell lysate was collected after gently shaking at room temperature for 15 min. The activity of Luciferase was determined by Flash & Glow LB955 tube luminometer. In the detection tube, 100 μL LAR II was added, and then 20 μL cell lysate was added to determine the Luciferase activity of firefly, and the fluorescence value was M1. Then, 100 μL Stop&Glo reagent was added to determine the activity of Renilla Luciferase, and the fluorescence value was M2. M1/M2 was defined as the relative activity of Luciferase measured after transfection.

Annexin V-fluorescein Isothiocyanate/Propidium Iodide (V-FITC/PI) Double Labeled Flow Cytometry for Detection of Apoptosis

After the treated cells reached the designated time, the cells were digested with trypsin. The digestion time should not be too long, and complete medium was added to terminate the reaction. The cells were rinsed twice with PBS, and the cells were counted, centrifuged at 1,500 rpm for 5 min, and 5×10^5 cells were collected for subsequent test. After that, 500 μL suspension was added to re-suspend cells, and 5 μL Annexin V-FITC was then added for mixing, followed by mixing with 10 μL PI, and the reaction was conducted at room temperature in the dark for 15 min. Within 1 h, the Annexin V-FITC fluorescence signal was detected by FL1 channel, while PI fluorescence signal was detected by FL2 or FL3 channel.

Statistical Analysis

All data in this study were processed by SPSS 21.0 statistical software (SPSS, IBM, Armonk, NY, USA). After normal distribution test and homogeneity test of variance, the measurement data with normal distribution and homogeneous variance were expressed by mean ± standard deviation, and the data of non-paired design were compared by independent sample *t*-test. One-way analysis of variance (ANOVA) was used for multi-group comparison, and Tukey's test was used for post-hoc test. The presence of statistical significance was determined with $p < 0.05$.

Results

Downregulated Expression of MiR-135a-5p in MI Mouse Model and Cell Hypoxia Model

It has been reported that miR-135a-5p was downregulated in many heart diseases, such as myocardial hypertrophy and pulmonary hypertension. In

our study, our authors proposed a hypothesis that miR-135a-5p might be involved in the progression of MI. Our authors intended to further explore the molecular mechanism of miR-135a-5p in MI.

First, the myocardial cell hypoxia model was to simulate the MI model *in vitro*. According to the results, compared with the Control group, there was significantly downregulated expression of miR-135a-5p in H9c2 cells of the Hypoxia group (Figure 1A), accompanied by markedly increased count of cell apoptosis detected by flow cytometry (Figure 1BC, $p<0.05$). Further-

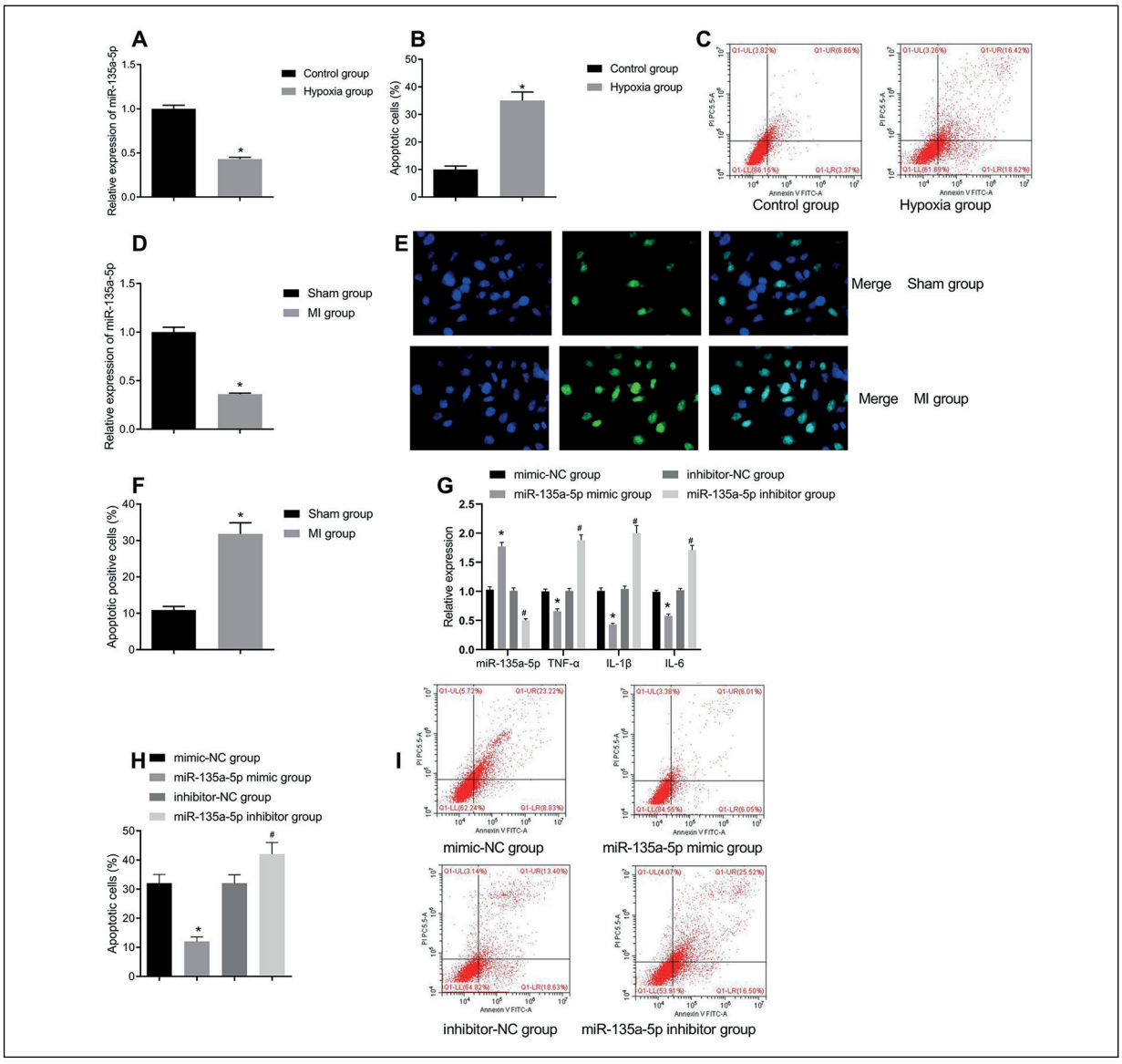

Figure 1. Downregulated expression of miR-135a-5p in MI mouse model and cell hypoxia model. Note: **A**, Expression of miR-135a-5p detected by qRT-PCR in myocardial cells before and after hypoxia treatment; **B**, Cell apoptosis comparison detected by flow cytometry in myocardial cells before and after hypoxia treatment; **C**, Cell apoptosis experimental results detected by flow cytometry in myocardial cells before and after hypoxia treatment; *compared with the Hypoxia group, $p<0.05$. **D**, Expression of miR-135a-5p detected by qRT-PCR in myocardial tissues before and after MI modeling; **E**, Apoptosis detected by TUNEL staining in myocardial tissues before and after MI modeling (magnification: 200X); **F**, Comparison of apoptotic positive cells obtained by TUNEL staining in myocardial tissues before and after MI modeling; *compared with the Control group, $p<0.05$. **G**, Expression of miR-135a-5p, TNF-α, IL-1β and IL-6 detected by qRT-PCR in myocardial cells after cell transfection based on the intervention of miR-135a-5p expression; **H**, Cell apoptosis experimental results detected by flow cytometry in myocardial cells after cell transfection based on the intervention of miR-135a-5p expression; **I**, Cell apoptosis comparison detected by flow cytometry in myocardial cells after cell transfection based on the intervention of miR-135a-5p expression; *compared with mimic-NC group, $p< 0.05$; #compared with inhibitor-NC group, $p< 0.05$.

more, in animal experiments, the apoptosis level of myocytes and the expression of miR-135a-5p were detected after MI. The results showed that the expression of miR-135a-5p in MI group was significantly lower than that in sham group (Figure 1D, $p<0.05$), and TUNEL showed that the number of apoptotic cells increased significantly (Figure 1EF, $p<0.05$). To further explore the effect of miR-135a-5p on myocardial cells, our study further overexpressed and knocked down miR-135a-5p in myocardial cells to evaluate the effect of miR-135a-5p on cell function under hypoxia. Considering the important role of inflammatory response in the process of MI, the expression of TNF-α, IL-1β and IL-6 was detected. The results showed that the levels of TNF-α, IL-1β and IL-6 in miR-135a-5p mimic group were significantly decreased compared with those of mimic-NC group, with increased expression of miR-135a-5p in the former group that suggested successful transfection (Figure 1G, $p<0.05$), associated with decreased count of cell apoptosis (Figure 1HI, $p<0.05$). Meanwhile, compared with inhibitor-NC group, miR-135a-5p inhibitor group showed significantly upregulated levels of TNF-α, IL-1β and IL-6 (Figure 1G, $p<0.05$), and significantly increased cell apoptosis (Figure 1HI, $p<0.05$), with decreased expression of miR-135a-5p to predict a successful transfection. Therefore, it was confirmed that under hypoxia stimulation, the expression of miR-135a-5p was significantly decreased; up-regulation of miR-135a-5p could reduce the inflammatory response after hypoxia treatment.

CXCL12 as a Target Gene of MiR-135a-5p to Affect Inflammatory Reaction and Myocardial Cell Apoptosis

To further study the downstream regulation mechanism of miR-135a-5p, it was predicted that CXCL12 can target miR-135a-5p through starBase online website, and there did exist binding regions between CXCL12 and miR-135a-5p (Figure 2A). It has been reported that the expression of CXCL12 in patients with unstable angina pectoris and acute MI is significantly increased. At the same time, based on the above results, it was speculated here that miR-135a-5p might regulate the expression of CXCL12 and then affect the function of myocardial cells. To further verify the targeting relationship between miR-135a-5p and CXCL12, Dual-Luciferase reporter gene assay was used in H9c2 cells. Corresponding results showed that compared with the control group, the luciferase activity of CXCL12 wild-type 3'UTR group was significantly decreased (Figure 2B, $p< 0.05$), yet without significant change in the Luciferase activity of CXCL12 mutant-type 3'UTR group ($p> 0.05$).

To further verify the effects of CXCL12 on inflammatory response and myocardial cell apoptosis, the expression of CXCL12 was detected in myocardial tissue of MI mice and hypoxia model cells. Corresponding results showed that compared with sham group, MI group had significantly upregulated expression of CXCL12 (Figure 2C, $p<0.05$); meanwhile, compared with Control group, the expression of CXCL12 increased significantly after hypoxia (Figure 2D, $p<0.05$). At the same time, further detection of apoptosis related factors of Bax and Bcl-2, as well as inflammatory factors of TNF-α, IL-1β and IL-6 (Figure 2E) showed that in hypoxia model, compared with sh-NC group, the expression of Bax in sh-CXCL12 group were decreased, and the expression of Bcl-2 was increased ($p<0.05$), while the levels of TNF-α, IL-1β and IL-6 were decreased ($p<0.05$). Moreover, flow cytometry showed that sh-CXCL12 group had reduced apoptosis level and inhibited apoptosis of myocardial cells after hypoxia than the sh-NC group ($p<0.05$); while oe-CXCL12 group showed the opposite trends of increased apoptosis level and increased apoptosis of myocardial cells after hypoxia in relative to oe-NC group ($p<0.05$).

To demonstrate that miR-135a-5p plays a role by regulating CXCL12, miR-135a-5p and CXCL12 were overexpressed and knocked down respectively. According to the results, in the hypoxia model, compared with the mimic-NC group, the expression of CXCL12 (Figure 2F, $p<0.05$) and the apoptosis of myocardial cells in miR-135a-5p mimic were significantly decreased (Figure 2GH, $p<0.05$); on the contrary, in relative to inhibitor-NC group, miR-135a-5p inhibitor group showed markedly increased expression of CXCL12 (Figure 2F, $p<0.05$) and the apoptosis of myocardial cells (Figure 2GH, $p<0.05$). In addition, compared with mimic NC+oe-NC group, miR-135a-5p mimic+oe-NC group showed decreased expression of CXCL12 and miR-135a-5p mimic+oe-CXCL12 group had no significant difference in the expression of CXCL12; while compared with miR-135a-5p mimic+oe-NC group, miR-135a-5p mimic+oe-CXCL12 group had evidently increased expression of CXCL12

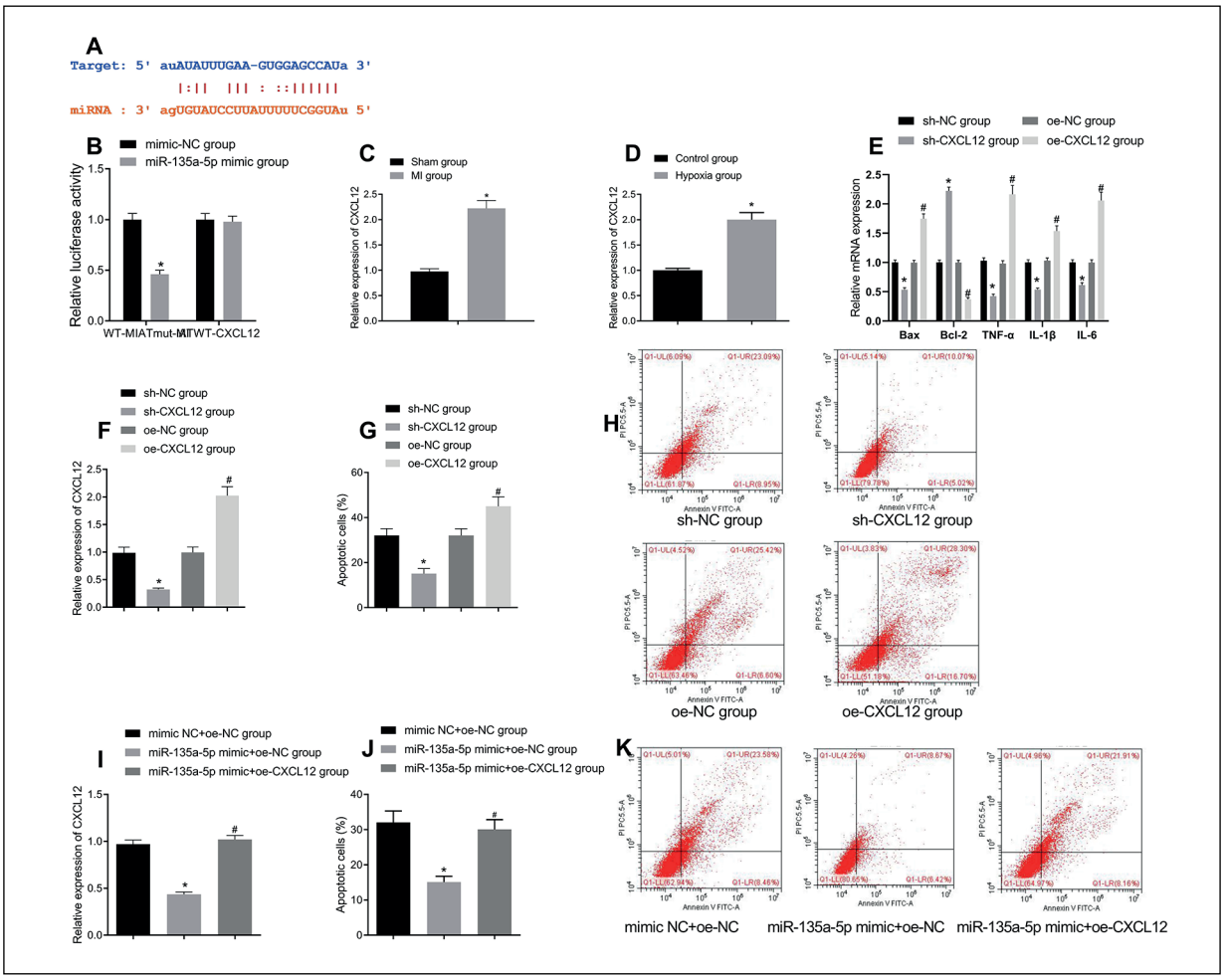

Figure 2. CXCL12 as a target gene of miR-135a-5p to affect inflammatory reaction and myocardial cell apoptosis Note: **A**, Prediction of the binding sites of miR-135a-5p and CXCL12 by using starBase; **B**, Verification of the targeting relationship between miR-135a-5p and CXCL12 by using dual luciferase reporter gene assay; **C**, Expression of CXCL12 detected by qRT-PCR in myocardial tissues before and after MI modeling; *compared with Shame group, $p< 0.05$. **D**, Expression of CXCL12 detected by qRT-PCR in myocardial cells before and after hypoxia treatment; *compared with Control group, $p< 0.05$. **E,** Expression of Bax, Bcl-2, TNF-α, IL-1β and IL-6 detected by qRT-PCR in myocardial cells after cell transfection based on the intervention of CXCL12 expression; **F**, Expression of CXCL12 detected by qRT-PCR in myocardial cells after cell transfection based on the intervention of CXCL12 expression; **G**, Cell apoptosis comparison detected by flow cytometry in myocardial cells after cell transfection based on the intervention of CXCL12 expression; **H**, Cell apoptosis experimental results detected by flow cytometry in myocardial cells after cell transfection based on the intervention of CXCL12 expression; *compared with sh-NC group, $p< 0.05$; #compared with oe-NC group, $p< 0.05$. **I**, Expression of CXCL12 detected by qRT-PCR in myocardial cells after cell transfection based on the intervention of both miR-135a-5p and CXCL12 expression; **J**, Cell apoptosis comparison detected by flow cytometry in myocardial cells after cell transfection based on the intervention of both miR-135a-5p and CXCL12 expression; **K**, Cell apoptosis experimental results detected by flow cytometry in myocardial cells after cell transfection based on the intervention of both miR-135a-5p and CXCL12 expression; *compared with mimic NC+oe-NC group, $p< 0.05$; #compared with miR-135a-5p mimic+oe-NC group, $p< 0.05$.

(Figure 2I, $p<0.05$) and the apoptosis of myocardial cells (Figure 2JK, $p<0.05$). Collectively, miR-135a-5p was involved in the protection of myocardial cells by negatively regulating the expression of CXCL12.

MiR-135a-5p Regulation of CXCL12 Expression and Mediation of the Activation of AK-STAT Signaling Pathway

The above results indicated the interaction between miR-135a-5p and CXCL12. In our

study, it was further speculated here that the downstream mechanism of miR-135a-5p regulating CXCL12 to mediate apoptosis was related to the activation of JAK-STAT signaling pathway.

To further verify this hypothesis, our study detected the expression of JAK2, STAT3, and corresponding phosphorylation levels (p-JAK2 and p-STAT3) in myocardial cells of the hypoxia model. Consequently, it was found that compared with mimic-NC group, miR-135a-5p mimic group showed decreased expression of p-JAK2 and p-STAT3 (p<0.05); miR-135a-5p inhibitor group had increased expression of p-JAK2 and p-STAT3 than the inhibitor-NC group (Figure 3A, p<0.05). Meanwhile, in relative to sh-NC group, sh-CXCL12 group revealed decreased expression of p-JAK2 and p-STAT3 (p<0.05); while compared with oe-NC group, oe-CXCL12 had increased expression of p-JAK2 and p-STAT3 (Figure 3B, p<0.05). In addition, compared with mimic NC+oe-NC group, miR-135a-5p mimic+oe-NC group had decreased expression of p-JAK2 and p-STAT3 (p<0.05), while no change was found in miR-135a-5p mimic+oe-CXCL12 group (p>0.05); while in relative to miR-135a-5p mimic+oe-NC group, miR-135a-5p mimic+oe-CXCL12 group revealed increased expression of p-JAK2 and p-STAT3 (Figure 3C, P<0.05). Moreover, there was no significant change in the expression of JAK2 and STAT3 in all groups (p>0.05). Therefore, these results showed that miR-135a-5p neg-

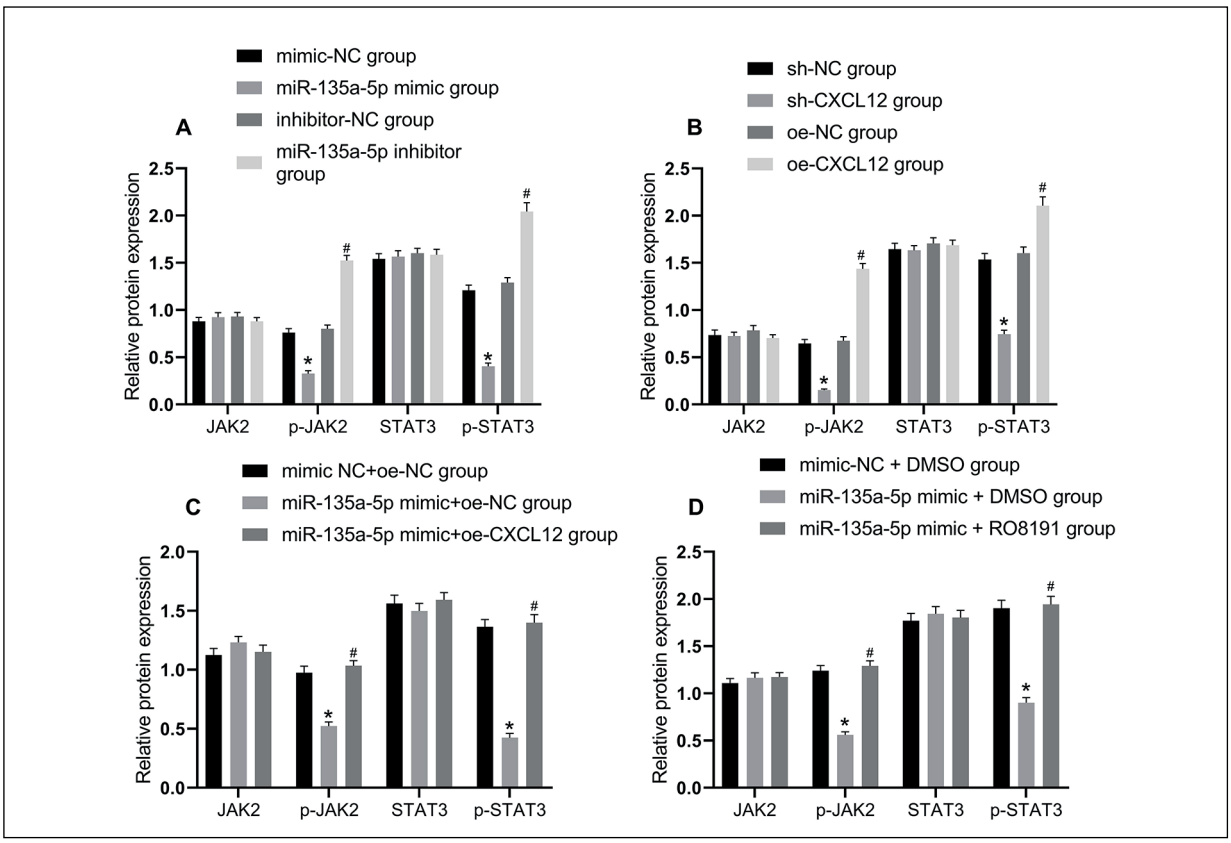

Figure 3. MiR-135a-5p regulation of CXCL12 expression and mediation of the activation of JAK-STAT signaling pathway. Note: **A**, Detection of JAK2, STAT3, p-JAK2 and p-STAT3 in myocardial cells of the hypoxia model after cell transfection based on the intervention of miR-135a-5p expression; *compared with mimic-NC group, p< 0.05; #compared with inhibitor-NC group, p< 0.05. **B**, Detection of JAK2, STAT3, p-JAK2 and p-STAT3 in myocardial cells of the hypoxia model after cell transfection based on the intervention of CXCL12 expression; *compared with sh-NC group, p< 0.05; #compared with oe-NC group, p< 0.05. **C**, Detection of JAK2, STAT3, p-JAK2 and p-STAT3 in myocardial cells of the hypoxia model after cell transfection based on the intervention of both miR-135a-5p and CXCL12 expression; *compared with mimic NC+oe-NC group, p< 0.05; #compared with miR-135a-5p mimic+oe-NC group, p< 0.05. **D**, Detection of JAK2, STAT3, p-JAK2 and p-STAT3 in myocardial cells of the hypoxia model after cell transfection based on the intervention of both miR-135a-5p expression and JAK-STAT signaling pathway; *compared with mimic-NC +DMSO group, p< 0.05; #compared with miR-135a-5p NC +DMSO group, p< 0.05.

atively regulated the expression of CXCL12 and inhibited the activation of JAK-STAT signaling pathway *in vitro*.

Furthermore, JAK2 agonist RO8191 was added for treatment of myocardial cells after miR-135a-5p mimic treatment. Western blot was used to detect the expression of JAK2, STAT3, p-jak2 and p-STAT3 in myocardial cells of the hypoxia model in each group. Compared with mimic-NC +DMSO group, miR-135a-5p mimic +DMSO group showed suppressed expression of p-JAK2 and p-STAT3 while there was no difference in their expression when compared with miR-135a-5p mimic +RO8191 group; meanwhile, in relative to miR-135a-5p mimic +DMSO group, miR-135a-5p mimic +RO8191 group had increased expression of p-JAK2 and p-STAT3 (Figure 3D, $p<0.05$); with no significant change in the expression of JAK2 and STAT3 ($p>0.05$). Therefore, these aforementioned results observed that miR-135a-5p negatively regulated the expression of CXCL12 and inhibited the activation of JAK-STAT signaling pathway in MI model.

Inhibition of the MiR-135a-5p/CXCL12/JAK-STAT Axial to Improve Myocardial Cell Apoptosis after MI in Mice

Our study further established a mouse model of MI to verify the role of miR-135a-5p/CXCL12/JAK-STAT axis *in vivo*. Mice were given tail vein injection and were divided into sh-NC group, sh-CXCL12 group, agomir-NC group and miR-135a-5p agomir group. HE staining showed that MI area appeared (Figure 4A), compared with sh-NC group, sh-CXCL12 group showed decreased MI area ($p<0.05$); and compared with agomir-NC group, miR-135a-5p-agomir also showed decreased MI area ($p<0.05$). Further detection of the expression of miR-135a-5p, CXCL12 and apoptosis related indexes showed that compared with sh-NC group and agomir-NC separately, miR-135a-5p-agomir group showed increased expression of miR-135a-5p, while sh-CXCL12 group had no change in miR-135a-5p (Figure 4B, $p>0.05$), and both groups had reduced expression of CXCL12 (Figure 4B, $p<0.05$), downregulated p-JAK2 and p-STAT3 protein expression (Figure 4BD, $p<0.05$), yet with no significant change in the protein expression of JAK2 and STAT3 ($p>0.05$), but with reduced levels of TNF-α, IL-1β and IL-6 (Figure 4C, $p<0.05$), decreased Bax expression and increased Bcl-2 expression (Figure 4C, $p<0.05$).

In addition, for additional verification of the role of miR-135a-5p/CXCL12/JAK-STAT, miR-135a-5p-agomir and pcDNA-CXCL12 were injected in mice. Compared with agomir-NC+pcDNA group, agomir-NC+pcDNA-CXCL12 group detected increased MI area (Figure 4E, $p<0.05$), no difference in miR-135a-5p expression (Figure 4F, $p>0.05$) but increase in CXCL12 expression (Figure 4F, $p<0.05$), increased p-JAK2 and p-STAT3 expression (Figure 4FH, $p<0.05$), increased TNF-α, IL-1β and IL-6 levels (Figure 4G, $p<0.05$), as well as upregulated Bax expression and downregulated Bcl-2 expression (Figure 4G, $p<0.05$); while there was no difference in miR-135a-5p-agomir+pcDNA-CXCL12 group. The above results confirmed the above cytological experiment, that was, under the condition of MI, inhibiting the miR-135a-5p/CXCL12/JAK-STAT axis can reduce the inflammatory reaction and reduce the apoptosis of myocardial cells.

Discussion

The most common cause of MI is coronary atherosclerosis that may induce vascular blockage and plaque rupture, which is characterized by endothelial damage, lipid accumulation and atherosclerotic plaque formation[32,33]. Subsequent myocardial cell necrosis and apoptosis caused by excessive inflammation constitute the primary causes of myocardial cell damage and loss. Apoptosis mainly occurs in the ischemic region[34]. Myocardial cell apoptosis plays an important role in the pathophysiological process of cardiac remodeling and heart failure after MI[35]. Reducing myocardial cell apoptosis has been proven to possess the capability to improve cardiac function and cardiac remodeling after MI[36]. Therefore, delaying inflammatory reaction, reducing apoptosis and inducing myocardial cell survival are the key to the treatment of MI[37]. In terms of the role of inflammation, there have been abundant previous studies *in vivo* and *in vitro*[38,39]. Ma et al[38] revealed that a high-sensitivity CRP level can be a key factor to carry out risk stratification for patients with acute coronary syndromes[38]. Besides, Zhang et al[39] carried out an experiment and revealed that oxidative stress and inflammation in human coronary artery endothelial cells can be attenuated by silencing PHACTR1 to alleviate the nuclear accumulation of p65 and NF-κB via interaction with MRTF-A[39]. Of course, in addition to inflammation, angiogenesis, hypoxia and growth factors are involved in the development of MI that deserves emphasis[40,41]. Despite clinical inter-

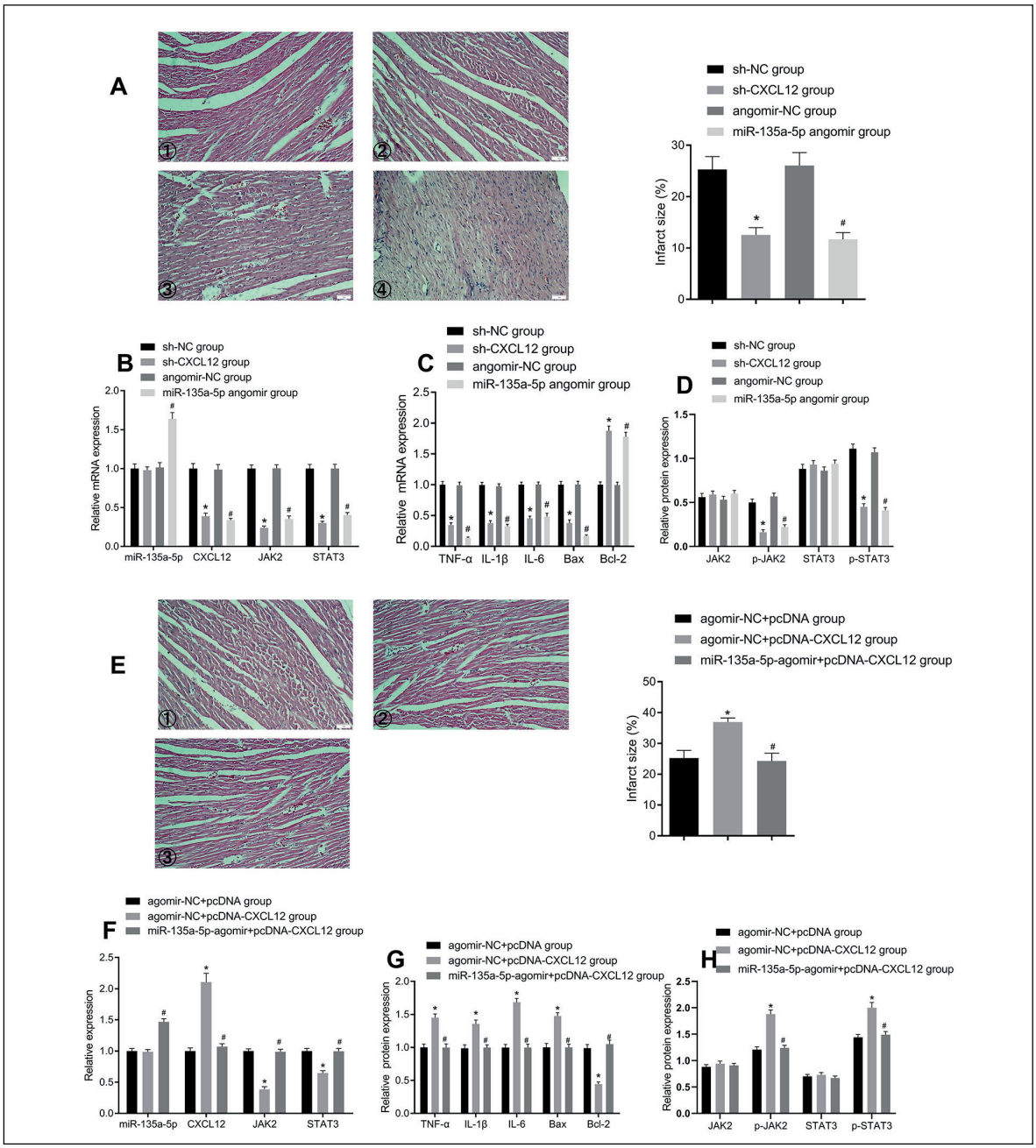

Figure 4. Inhibition of the miR-135a-5p/CXCL12/JAK-STAT axial to improve myocardial cell apoptosis after MI in mice. Note: **A**, MI area verified by HE staining ((1)sh-NC, (2) sh-CXCL12, (3) agomir-NC and (4) miR-135a-5p agomir) and statistical comparison after injection of sh-NC, sh-CXCL12, agomir-NC and miR-135a-5p agomir (magnification: 200×); **B**, qRT-PCR detection of miR-135a-5p, CXCL12 and JAK2 and STAT3 after injection of sh-NC, sh-CXCL12, agomir-NC and miR-135a-5p agomir; **C**, qRT-PCR detection of TNF-α, IL-1β, IL-6, Bax and Bcl-2 after injection of sh-NC, sh-CXCL12, agomir-NC and miR-135a-5p agomir; **D**, Western blot detection of JAK2/p-JAK2 and STAT3/p-STAT3 after injection of sh-NC, sh-CXCL12, agomir-NC and miR-135a-5p agomir; *compared with sh-NC group, $p<0.05$; #compared with agomir-NC group, $p< 0.05$. **E**, MI area verified by HE staining (1)agomir-NC+pcDNA, (2) agomir-NC+pcDNA-CXCL12 and (3) miR-135a-5p-agomir+pcDNA-CXCL12) and statistical comparison after injection of agomir-NC+pcDNA, agomir-NC+pcDNA-CXCL12 and miR-135a-5p-agomir+pcDNA-CXCL12 (magnification: 200×); **F**, qRT-PCR detection of miR-135a-5p, CXCL12 and JAK2 and STAT3 after injection of agomir-NC+pcDNA, agomir-NC+pcDNA-CXCL12 and miR-135a-5p-agomir+pcDNA-CXCL12; **G,** qRT-PCR detection of TNF-α, IL-1β, IL-6, Bax and Bcl-2 after injection of agomir-NC+pcDNA, agomir-NC+pcDNA-CXCL12 and miR-135a-5p-agomir+pcDNA-CXCL12; **H,** Western blot detection of JAK2/p-JAK2 and STAT3/p-STAT3 after injection of agomir-NC+pcDNA, agomir-NC+pcDNA-CXCL12 and miR-135a-5p-agomir+pcDNA-CXCL12; *compared with agomir-NC+pcDNA group, $p< 0.05$; #compared with agomir-NC+pcDNA-CXCL12 group, $p< 0.05$.

vention such as thrombolysis and other methods for the treatment of MI, its mortality is still high with the presence of long-term complications. It is urgent to find a new therapeutic approach to relieve the current situation. Recent discovery and investigation of the new class of regulatory factors, miRNAs for example, play a regulatory role in different biological processes, including apoptosis, fibrosis, inflammation, angiogenesis and repair[42,43].

Specifically, miRNA research has rapidly developed into a mature and extensive field. In fact, most of the genome (about 60%) is regulated by miRNAs. The regulation level of some miRNAs after MI may help to reduce cell apoptosis, inhibit tissue damage, promote neovascularization, control the degree of ventricular wall fibrosis, thus improving the long-term prognosis[44]. Of note, miR-135 plays an important role in many kinds of tumors and malignant diseases[45]. There are four kinds of mature human miR-135 family, including miR-135a-5p. By targeting and silencing the target genes, miR-135 can provide a more detailed basis for clinical treatment of replication patients by targeting the effects of target genes on cell proliferation, invasion, migration, apoptosis, angiogenesis, chemotherapy resistance and evaluation of patients' prognosis[46,47]. However, the complex regulatory network between miRNA and mRNA also poses new challenges for the progress of cancer research. How to quickly and efficiently screen the most closely related factors with the occurrence and development of diseases is a key problem to be addressed urgently. In general, miRNAs play biological effects by regulating the expression of one or a group of target genes. Therefore, we predicted in this study the target genes of miR-135a-5p by biological techniques. CXCL12 gene has attracted our attention for the following reasons. First of all, our team predicted that CXCL12 mRNA3'UTR has a potential binding site complementary to miR-135a-5p sequence, which can complement miR-135a-5p, suggesting that CXCL12 is a natural target gene of miR-135a-5p. Secondly, CXCL12 is a pleiotropic chemokine, which is widely expressed in many tissues, such as bone marrow stem cells, endothelial cells, heart, skeletal muscle, liver, brain tissue, kidney parenchyma cells and osteoblasts[48]. Previous evidence has supported that CXCL12 also functions significantly in the repair of myocardial cells, angiogenesis and the recovery of left ventricular function after MI[49,50]. In addition, the abnormal expression and function of other members of CXC chemokine family have been documented to exert a critical role in the occurrence and development of cardiovascular diseases[51,52]. At the same time, CXCL12 was predicted as a related factor of JAK-STAT signaling pathway by biological website in our pre-experiment stage. It is worth noting that JAK-STAT signaling pathway is one of the most widely studied signaling pathways. As mentioned above, JAK-STAT signaling pathway is found to be involved significantly in the development of human diseases. It is an important pathway of cytokine signaling. It is responsible for the direct transmission of the stimulatory signals on the cell membrane to the nucleus, and then activate the target gene transcription to regulate cell stress response, apoptosis, inflammatory response and other biological effects[53-55]. Hence, the present study was carried out to explore the regulatory role of miR-135a-5p/CXCL12/JAK-STAT signaling axis in MI.

In this study, a mouse model of MI was established. HE staining was used to indicate the success of the animal experiment. TUNEL test showed the existence of apoptosis in ischemic region. In order to make the results more convincing, we also established H9c2 myocardial cell hypoxia model. The results are as follows. There was markedly downregulated expression of miR-135a-5p in both animal MI and cell hypoxia models, with significantly increased apoptosis levels. Meanwhile, considering the important role of inflammatory response in the process of MI, the expression of TNF-α, IL-1β and IL-6 was detected, all of which were essential inflammatory indexes. It was found that TNF-α, IL-1β and IL-6 can be decreased by miR-135a-5p mimic treatment, but increased by miR-135a-5p inhibitor treatment, suggesting that up-regulation of miR-135a-5p could reduce the inflammatory response after hypoxia treatment. Furthermore, with the identification of the targeting relationship between miR-135a-5p and CXCL12, the expression of CXCL12 was detected in myocardial tissue of MI mice and hypoxia model cells to further verify the effects of CXCL12 on inflammatory response and myocardial cell apoptosis. It was discovered that silenced expression of CXCL12 could decrease the expression of TNF-α, IL-1β IL-6 and Bax, while increase Bcl-2 expression, with an opposite trend found after overexpressing CXCL12. To demonstrate that miR-135a-5p plays a role by regulating CXCL12, our subsequent experiment was continued with the discovery of reduced CX-

CL12 research and apoptosis after overexpressing miR-135a-5p, but higher CXCL12 expression and apoptosis after inhibiting miR-135a-5p. More importantly, overexpression of CXCL12 reversed the beneficial role of miR-135a-5p in the apoptosis of myocardial cells. It can hence be speculated preliminarily that miR-135a-5p has a role in the protection of myocardial cells by negatively regulating CXCL12 expression.

Furthermore, our study found that miR-135a-5p regulating CXCL12 to mediate apoptosis was related to the activation of JAK-STAT signaling pathway, which was proven by the detection of suppressed phosphorylated levels of JAK and STAT. It may suggest that the mechanism of miR-135a-5p regulating CXCL12 may be associated with the regulation of the phosphorylation of JAK and STAT. Besides, a reverse research in hypoxia model indicated that activation of JAK-STAT signaling pathway resulted in the counteraction of the positive role of miR-135a-5p overexpression and silenced CXCL12 expression. Therefore, it could be confirmed with a cautious manner that miR-135a-5p negatively regulated the expression of CXCL12 and inhibited the activation of JAK-STAT signaling pathway to exert a positive protective role in MI model. Simultaneously, for an in-depth and comprehensive identification, our subsequent experiment related to animal MI model indicated that overexpression of miR-135a-5p and silenced CXCL12 expression contributed to the reduced MI area and inhibited activation of JAK-STAT signaling pathway, as well as suppressed levels of inflammatory indexes and intervened levels of apoptotic indexes. Meanwhile, a reverse research in animal MI model revealed that overexpression of CXCL12 using pcDNA-CXCL12 treatment after overexpression of miR-135a-5p using miR-135a-5p-agomir led to increased MI area, activated JAK-STAT signaling pathway, increased TNF-α, IL-1β and IL-6 levels, upregulated Bax expression and downregulated Bcl-2 expression.

Conclusions

Collectively, our study for the first time confirms that the miR-135a-5p/CXCL12/JAK-STAT signaling axis can reduce inflammatory reaction and reduce the apoptosis of myocardial cells form the aspects of hypoxia treatment and animal MI model construction, which may be related to the mechanism that miR-135a-5p overexpression inhibits the expression of CXCL12 to alleviate inflammatory reaction and suppress cell apoptosis via the inhibited activation of JAK-STAT signaling pathway to suppress the phosphorylation of JAK and STAT. Innovatively, our research constructed two experimental models of *in vitro* myocardial cell hypoxia model and *in vivo* mouse MI model to explain the interaction of miR-135a-5p and its downstream target gene of CXCL12/ signaling pathway of JAK-STAT involved in protecting the progression of MI. Besides, on the basis of adenovirus vector and plasmid transfection, our study established a complex grouping design to verify the role of miR-135a and CXCL12 overexpression and silenced expression as well as the activation of JAK-STAT comprehensively. This study provides an abundant and scientific evidence to understand the mechanism of MI, and may provide new insight in searching for potential therapeutic approaches for the treatment of cardiovascular diseases.

Conflict of Interest

The Authors declare that they have no conflict of interests.

Fund

This study was funded by Luoyang Science and Technology Plan (Medical Care and Health) Project (1603002A-5).

References

1) Gabriel-Costa D. The pathophysiology of myocardial infarction-induced heart failure. Pathophysiology 2018; 25: 277-284.
2) Zimarino M, Affinito V. The prognosis of periprocedural myocardial infarction after percutaneous coronary interventions. Cardiovasc Revasc Med 2013; 14: 32-36.
3) Fang J, Wang J, Chen F, Xu Y, Zhang H, Wang Y. α7nAChR deletion aggravates myocardial infarction and enhances systemic inflammatory reaction via mtor-signaling-related autophagy. Inflammation 2019; 42: 1190-1202.
4) Zhang M, Cheng YJ, Sara JD, Liu LJ, Liu LP, Zhao X, Gao H. Circulating microRNA-145 is associated with acute myocardial infarction and heart failure. Chin Med J (Engl) 2017; 130: 51-56.
5) Sayed AS, Xia K, Salma U, Yang T, Peng J. Diagnosis, prognosis and therapeutic role of circulating miRNAs in cardiovascular diseases. Heart Lung Circ 2014; 23: 503-510

6) Guo H, Ingolia NT, Weissman JS, Bartel DP. Mammalian microRNAs predominantly act to decrease target mRNA levels. Nature 2010; 466: 835-840.

7) Liu J, Dang L, Wu X, Li D, Ren Q, Lu A, Zhang G. MicroRNA-mediated regulation of bone remodeling: a brief review. JBMR Plus 2019; 3: e10213.

8) Schramedei K, Mörbt N, Pfeifer G, Läuter J, Rosolowski M, Tomm JM, von Bergen M, Horn F, Brocke-Heidrich K. MicroRNA-21 targets tumor suppressor genes ANP32A and SMARCA4. Oncogene 2011; 30: 2975-2985.

9) Nouraee N, Mowla SJ. MiRNA therapeutics in cardiovascular diseases: promises and problems. Front Genet 2015; 6: 232.

10) de Lucia C, Komici K, Borghetti G, Femminella GD, Bencivenga L, Cannavo A, Corbi G, Ferrara N, Houser SR, Koch WJ, Rengo G. MicroRNA in cardiovascular aging and age-related cardiovascular diseases. Front Med (Lausanne) 2017; 4: 74.

11) Cai W, Zhang Y, Su Z. ciRS-7 targeting miR-135a-5p promotes neuropathic pain in CCI rats via inflammation and autophagy. Gene 2020; 736: 144386.

12) Kim D, Kim J, Yoon JH, Ghim J, Yea K, Song P, Park S, Lee A, Hong CP, Jang MS, Kwon Y, Park S, Jang MH, Berggren PO, Suh PG, Ryu SH. CXCL12 secreted from adipose tissue recruits macrophages and induces insulin resistance in mice. Diabetologia 2014; 57: 1456-1465.

13) Guyon A. CXCL12 chemokine and its receptors as major players in the interactions between immune and nervous systems. Front Cell Neurosci 2014; 8: 65.

14) Qiao N, Wang L, Wang T, Li H. Inflammatory CXCL12-CXCR4/CXCR7 axis mediates G-protein signaling pathway to influence the invasion and migration of nasopharyngeal carcinoma cells. Tumour Biol 2016; 37: 8169-8179.

15) Grdović N, Rajić J, Petrović SM, Dinić S, Uskoković A, Mihailović M, Jovanović JA, Tolić A, Pucar A, Milašin J, Vidaković M. Association of CXCL12 gene promoter methylation with periodontitis in patients with diabetes mellitus type 2. Arch Oral Biol 2016; 72: 124-133.

16) Smith JM, Johanesen PA, Wendt MK, Binion DG, Dwinell MB. CXCL12 activation of CXCR4 regulates mucosal host defense through stimulation of epithelial cell migration and promotion of intestinal barrier integrity. Am J Physiol Gastrointest Liver Physiol 2005; 288: G316-G326.

17) Damås JK, Waehre T, Yndestad A, Ueland T, Müller F, Eiken HG, Holm AM, Halvorsen B, Frøland SS, Gullestad L, Aukrust P. Stromal cell-derived factor-1alpha in unstable angina: potential antiinflammatory and matrix-stabilizing effects. Circulation 2002; 106: 36-42.

18) Mehta NN, Matthews GJ, Krishnamoorthy P, Shah R, McLaughlin C, Patel P, Budoff M, Chen J, Wolman M, Go A, He J, Kanetsky PA, Master SR, Rader DJ, Raj D, Gadegbeku CA, Shah R, Schreiber M, Fischer MJ, Townsend RR, Kusek J, Feldman HI, Foulkes AS, Reilly MP, Chronic Renal Insufficiency Cohort (CRIC) Study Investigators. Higher plasma CXCL12 levels predict incident myocardial infarction and death in chronic kidney disease: findings from the Chronic Renal Insufficiency Cohort study. Eur Heart J 2014; 35: 2115-2122.

19) Fu WB, Wang WE, Zeng CY. Wnt signaling pathways in myocardial infarction and the therapeutic effects of Wnt pathway inhibitors. Acta Pharmacol Sin 2019; 40: 9-12.

20) Chen B, Huang S, Su Y, Wu YJ, Hanna A, Brickshawana A, Graff J, Frangogiannis NG. Macrophage Smad3 protects the infarcted heart, stimulating phagocytosis and regulating inflammation. Circ Res 2019; 125: 55-70.

21) Fu WB, Wang WE, Zeng CY. Wnt signaling pathways in myocardial infarction and the therapeutic effects of Wnt pathway inhibitors. Acta Pharmacol Sin 2019; 40: 9-12.

22) Cheng S, Zhang X, Feng Q, Chen J, Shen L, Yu P, Yang L, Chen D, Zhang H, Sun W, Chen X. Astragaloside IV exerts angiogenesis and cardioprotection after myocardial infarction via regulating PTEN/PI3K/Akt signaling pathway. Life Sci 2019; 227: 82-93.

23) Fan YZ, Huang H, Wang S, Tan GJ, Zhang QZ. Effect of lncRNA MALAT1 on rats with myocardial infarction through regulating ERK/MAPK signaling pathway. Eur Rev Med Pharmacol Sci 2019; 23: 9041-9049.

24) Seif F, Khoshmirsafa M, Aazami H, Mohsenzadegan M, Sedighi G, Bahar M. The role of JAK-STAT signaling pathway and its regulators in the fate of T helper cells. Cell Commun Signal 2017; 15: 23.

25) Niu GJ, Xu JD, Yuan WJ, Sun JJ, Yang MC, He ZH, Zhao XF, Wang JX. Protein inhibitor of activated STAT (PIAS) negatively regulates the JAK/STAT Pathway by Inhibiting STAT phosphorylation and Translocation. Front Immunol 2018; 9: 2392.

26) Mirenda M, Toffali L, Montresor A, Scardoni G, Sorio C, Laudanna C. Protein tyrosine phosphatase receptor type γ is a JAK phosphatase and negatively regulates leukocyte integrin activation. J Immunol 2015; 194: 2168-2179.

27) Serra D, Rufino AT, Mendes AF, Almeida LM, Dinis TC. Resveratrol modulates cytokine-induced Jak/STAT activation more efficiently than 5-aminosalicylic acid: an in vitro approach. PLoS One 2014; 9: e109048.

28) Subramaniam A, Shanmugam MK, Perumal E, Li F, Nachiyappan A, Dai X, Swamy SN, Ahn KS, Kumar AP, Tan BKH, Hui KM, Sethi G. Potential role of signal transducer and activator of transcription (STAT)3 signaling pathway in inflammation, survival, proliferation and invasion of hepatocellular carcinoma. Biochim Biophys Acta 2013; 1835: 46-60.

29) Booz GW, Day JN, Baker KM. Interplay between the cardiac renin angiotensin system and JAK-STAT signaling: role in cardiac hypertrophy, ischemia/reperfusion dysfunction, and heart failure. J Mol Cell Cardiol 2002; 34: 1443-1453.

30) Yadav M, Kumari P, Yadav V, Kumar S. Pharmacological preconditioning with phosphodiestrase inhibitor: an answer to stem cell survival against ischemic injury through JAK/STAT signaling. Heart Fail Rev 2020; 25: 355-366.

31) Gong P, Zhang Z, Zou Y, Tian Q, Han S, Xu Z, Liao J, Gao L, Chen Q, Li M. Tetramethylpyrazine attenuates blood-brain barrier disruption in ischemia/reperfusion injury through the JAK/STAT signaling pathway. Eur J Pharmacol 2019; 854: 289-297.

32) Tamis-Holland JE, Jneid H, Reynolds HR, Agewall S, Brilakis ES, Brown TM, Lerman A, Cushman M, Kumbhani DJ, Arslanian-Engoren C, Bolger AF, Beltrame JF, American Heart Association Interventional Cardiovascular Care Committee of the Council on Clinical Cardiology; Council on Cardiovascular and Stroke Nursing; Council on Epidemiology and Prevention; and Council on Quality of Care and Outcomes Research. Contemporary Diagnosis and Management of Patients With Myocardial Infarction in the Absence of Obstructive Coronary Artery Disease: A Scientific Statement From the American Heart Association. Circulation 2019; 139: e891-e908.

33) Calais F, Eriksson Östman M, Hedberg P, Rosenblad A, Leppert J, Fröbert O. Incremental prognostic value of coronary and systemic atherosclerosis after myocardial infarction. Int J Cardiol 2018; 261: 6-11.

34) Yao H, Han X, Han X. The cardioprotection of the insulin-mediated PI3K/Akt/mTOR signaling pathway. Am J Cardiovasc Drugs 2014; 14: 433-442.

35) Wang X, Guo Z, Ding Z, Mehta JL. Inflammation, autophagy, and apoptosis after myocardial Infarction. J Am Heart Assoc 2018; 7: e008024.

36) Ren L, Chen S, Liu W, Hou P, Sun W, Yan H. Down-regulation of long non-coding RNA nuclear enriched abundant transcript 1 promotes cell proliferation and inhibits cell apoptosis by targeting miR-193a in myocardial ischemia/reperfusion injury. BMC Cardiovasc Disord 2019; 19: 192.

37) He F, Liu H, Guo J, Yang D, Yu Y, Yu J, Yan X, Hu J, Du Z. Inhibition of microRNA-124 reduces cardiomyocyte apoptosis following myocardial infarction via targeting STAT3. Cell Physiol Biochem 2018; 51: 186-200.

38) Ma QQ, Yang XJ, Yang NQ, Liu L, Li XD, Zhu K, Fu Q, Wei P. Study on the levels of uric acid and high-sensitivity C-reactive protein in ACS patients and their relationships with the extent of the coronary artery lesion. Eur Rev Med Pharmacol Sci 2016; 20: 4294-4298.

39) Zhang Z, Jiang F, Zeng L, Wang X, Tu S. PHACTR1 regulates oxidative stress and inflammation to coronary artery endothelial cells via interaction with NF-κB/p65. Atherosclerosis. 2018; 278: 180-189.

40) Du Y, Ge Y, Xu Z, Aa N, Gu X, Meng H, Lin Z, Zhu D, Shi J, Zhuang R, Wu X, Wang X, Yang Z. Hypoxia-inducible factor 1 alpha (HIF-1α)/vascular endothelial growth factor (VEGF) pathway participates in angiogenesis of myocardial infarction in muscone-treated mice: preliminary study. Med Sci Monit 2018; 24: 8870-8877.

41) Li SN, Li P, Liu WH, Shang JJ, Qiu SL, Zhou MX, Liu HX. Danhong injection enhances angiogenesis after myocardial infarction by activating MiR-126/ERK/VEGF pathway. Biomed Pharmacother 2019; 120: 109538.

42) Xiao Y, Zhao J, Tuazon JP, Borlongan CV, Yu G. MicroRNA-133a and Myocardial Infarction. Cell Transplant 2019; 28: 831-838.

43) Chen J, Li C, Liu W, Yan B, Hu X, Yang F. miRNA-155 silencing reduces sciatic nerve injury in diabetic peripheral neuropathy. J Mol Endocrinol 2019; 63: 227-238.

44) Hu S, Huang M, Nguyen PK, Gong Y, Li Z, Jia F, Lan F, Liu J, Nag D, Robbins RC, Wu JC. Novel microRNA prosurvival cocktail for improving engraftment and function of cardiac progenitor cell transplantation. Circulation 2011; 124: S27-S34.

45) Taipaleenmäki H, Browne G, Akech J, Zustin J, van Wijnen AJ, Stein JL, Hesse E, Stein GS, Lian JB. Targeting of Runx2 by miR-135 and miR-203 impairs progression of breast cancer and metastatic bone disease. Cancer Res 2015; 75: 1433-1444.

46) Wang N, Zhang T. Downregulation of MicroRNA-135 promotes sensitivity of non-small cell lung cancer to gefitinib by targeting TRIM16. Oncol Res 2018; 26: 1005-1014.

47) Zheng Y, Zheng B, Meng X, Yan Y, He J, Liu Y. LncRNA DANCR promotes the proliferation, migration, and invasion of tongue squamous cell carcinoma cells through miR-135a-5p/KLF8 axis. Cancer Cell Int 2019; 19: 302.

48) Nazari A, Khorramdelazad H, Hassanshahi G. Biological/pathological functions of the CXCL12/CXCR4/CXCR7 axes in the pathogenesis of bladder cancer. Int J Clin Oncol 2017; 22: 991-1000.

49) Di Maggio S, Milano G, De Marchis F, D'Ambrosio A, Bertolotti M, Palacios BS, Badi I, Sommariva E, Pompilio G, Capogrossi MC, Raucci A. Non-oxidizable HMGB1 induces cardiac fibroblasts migration via CXCR4 in a CXCL12-independent manner and worsens tissue remodeling after myocardial infarction. Biochim Biophys Acta Mol Basis Dis 2017; 1863: 2693-2704.

50) Yang L, Yan F, Ma J, Zhang J, Liu L, Guan L, Zheng H, Li T, Liang D, Mu Y. Ultrasound-targeted microbubble destruction-mediated co-delivery of Cxcl12 (Sdf-1alpha) and Bmp2 Genes for myocardial repair. J Biomed Nanotechnol 2019; 15: 1299-1312.

51) Altara R, Manca M, Brandão RD, Zeidan A, Booz GW, Zouein FA. Emerging importance of chemokine receptor CXCR3 and its ligands in cardiovascular diseases. Clin Sci (Lond) 2016; 130: 463-478.

52) Connell BJ, Gordon JR, Saleh TM. ELR-CXC chemokine antagonism is neuroprotective in a

rat model of ischemic stroke. Neurosci Lett 2015; 606: 117-122.

53) Meares GP, Liu Y, Rajbhandari R, Qin H, Nozell SE, Mobley JA, Corbett JA, Benveniste EN. PERK-dependent activation of JAK1 and STAT3 contributes to endoplasmic reticulum stress-induced inflammation. Mol Cell Biol 2014; 34: 3911-3925.

54) Liu Q, Liang X, Liang M, Qin R, Qin F, Wang X. Ellagic acid ameliorates renal ischemic-reperfusion injury through NOX4/JAK/STAT Signaling Pathway. Inflammation 2020; 43: 298-309.

55) Malemud CJ. Negative regulators of JAK/STAT signaling in rheumatoid arthritis and osteoarthritis. Int J Mol Sci 2017; 18: 484.